International Journal of GEOMATE, Dec., 2025 Vol.29, Issue 136, pp.49-58
ISSN: 2186-2982 (P), 2186-2990 (O), Japan, DOI: https://doi.org/10.21660/2025.136.5203
Geotechnique, Construction Materials and Environment

TSUNAMI HAZARD ASSESSMENT DUE TO POTENTIAL EARTHQUAKE ALONG THE FLORES BACK ARC THRUST IN BULELENG REGENCY

Lestari Naomi Lydia Pandiangan[1,3], *Djati Mardiatno[2], Daryono[3] and Tomy Gunawan[3]

[1]Doctoral Program in Geography, Faculty of Geography, Universitas Gadjah Mada, Yogyakarta, Indonesia
[2]Center for Environmental Studies (PSLH) Universitas Gadjah Mada, Yogyakarta, Indonesia
[3]Agency for Meteorology Climatology and Geophysics (BMKG), Indonesia

*Corresponding Author, Received: 28 Aug. 2025, Revised: 26 Sep. 2025, Accepted: 09 Oct. 2025

ABSTRACT: Buleleng Regency in North Bali was considered to be widely prone to tsunamis, as it is in close vicinity to the active tectonic zone of the Flores Back-Arc Thrust that can lead to massive earthquakes. Flood area, maximum run-up height, and wave arrival time are the three critical seismic parameters analyzed in this research to assess tsunami risk in the studied region. This study used the COMCOT v1.7 software to perform numerical simulations for a hypothetical Mw 7.5 earthquake, incorporating both all-land and all-water data. The result shows that Gerokgak sub-district, which had the most inundated area, about 8.87 km², and the other sub-districts, such as Buleleng, Banjar, and Sawan, also faced inundation. At moderate water depths (0.5–3 m), the most extensive inundated areas overlap frequently with high-density populated coastal areas, particularly at the river outlets and lowlands. From the arrival time analysis, it is found that the eastern coast has the shortest warning time, e.g., the tsunami arrives at Ponjok Batu Beach 1 min 46 s after the triggering event, while the highest tsunami run-up value occurs at Bukti Beach (Kubu Tambahan), which is 9.86 m. Conversely, areas in the west, such as Gilimanuk, experience a tsunami arrival time exceeding 20 minutes. According to the results, the improvement of tsunami preparedness that includes early warning, evacuation planning, and coastal land use planning is necessary. The results of this study provide critical information for risk reduction strategies in Buleleng and similar coastal places.

Keywords: Numerical simulation, Run-up height, COMCOT, Inundation mapping, Wave arrival time

1. INTRODUCTION

Indonesia is located at the boundary of the Indo-Australian, Pacific, and Eurasian plates, forming subduction zones and numerous active faults [1][2]. The tectonic setting places Indonesia among the highest seismic-risk countries [3].

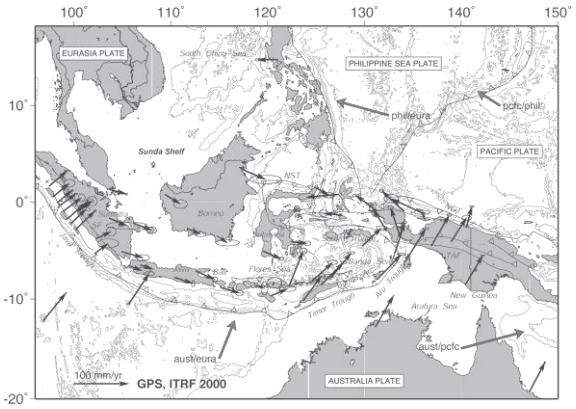

Fig. 1 Tectonic Map of Indonesia (Source: Bock, 2003)

Bali Island, particularly Buleleng Regency on its northern coast with a 157 km coastline, has complex tectonic settings and a high level of vulnerability to tsunamis [4]. The rapid development of coastal tourism also increases exposure [5], and social–spatial risk assessments are still limited in number [6]. The Indo-Australian Plate is subducting beneath the Sunda Plate at about 7 cm/year [7], pushing back-arc thrusting north of Bali [8]. The Flores Back Arc Thrust Zone is shown in Figure 2. The main sources include the Flores Back Arc Thrust (FBT), which stretches from Flores to northern Bali [9].

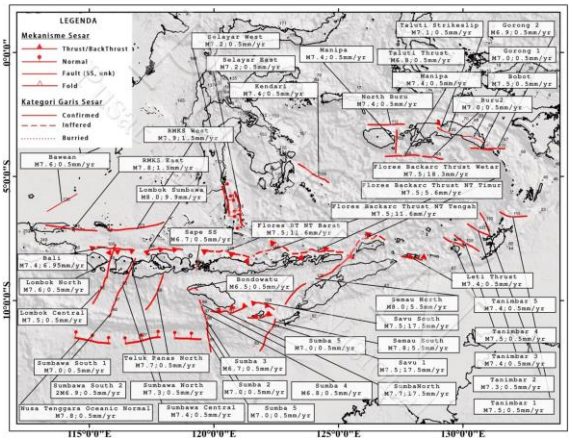

Fig. 2 Map of earthquake sources in Bali, Nusa Tenggara, and the Banda Sea (Source: PUSGEN, 2017)

Tsunamis generated by the Flores Back-Arc Thrust (FBT) zone have previously hit some coastlines in Buleleng Regency. Great Tsunamis of North Bali, 1815: This tsunami of North Bali happened on the 22nd of November with a magnitude of 7.3. This tragedy alone killed 10,253 victims in Singaraja and Buleleng. The 1818 North Bali earthquake produced a 3.5-m-high tsunami; the 1857 North Bali earthquake on 13 May generated a 3.4-m-high tsunami and resulted in 36 casualties, and the 1917 North Bali earthquake on 21 January resulted in a 2-m-high tsunami, killing 1,500 people in Buleleng, Jembrana, and Tabanan [10][11].

GIS-based hazard mapping and numerical modeling have been widely applied, with key parameters such as run-up, beach slope, and surface roughness [12]. Reliable research information on the risk of tsunamis at the study site is used to develop plans for improvement in the event of a tsunami [13]. Previous studies include evacuation route modeling on the south coast of Java using TUNAMI-N3 [14], tsunami energy assessment in the Sulawesi Sea [15], and risk studies in Kulon Progo [16]. More recently, COMCOT has been applied to simulate tsunami propagation, run-up, and inundation with high accuracy [17] and is recommended by IOC-UNESCO for tsunami analysis.

Based on this background, the present study investigates tsunami hazards in Buleleng Regency using the COMCOT v1.7 model, focusing on two research questions:

1. What is the tsunami run-up maximum along the coast of Buleleng?
2. How long does it take for a tsunami to reach the coast of many different locations along the coast?

The objective is to analyze inundation, run-up, and arrival times as a scientific basis for evacuation planning and disaster risk reduction in Buleleng [18].

Next, the present article moves on to discuss the literature covering tsunami definitions, essential variables, and inundation modelling. The method section, follows, describing the area of study, data applied and the earthquake source parameters. The results and discussion will describe the tsunami simulation in terms of wave propagation, arrival time, wave height, and inundation area for a number of sub-districts. Lastly, the paper will make a conclusion of findings and discuss its implication to Buleleng Disaster Risk Reduction.

2. RESEARCH SIGNIFICANCE

This study is significant in that it is the first thorough tsunami hazard assessment of Buleleng Regency under a scenario involving Flores Back-Arc Thrust earthquake. Integrating numerical modeling with spatial vulnerability analysis, the study enhances current understanding of tsunami risk in North Bali, which has been relatively underresearched before. The findings offer practical application for disaster risk reduction through informing early warning planning, evacuation planning, and coastal zoning controls and thereby promoting the resilience of communities and supporting evidence-based decision making for local governments.

3. METHODS

3.1 Study area

The research was conducted on beaches in Buleleng Regency. The observation points of the tsunami run-up are shown as the red triangles in Fig. 3. The regency's 16 areas of observation are where garbage is likely to accumulate, such as tourist sites, ports, and residential districts.

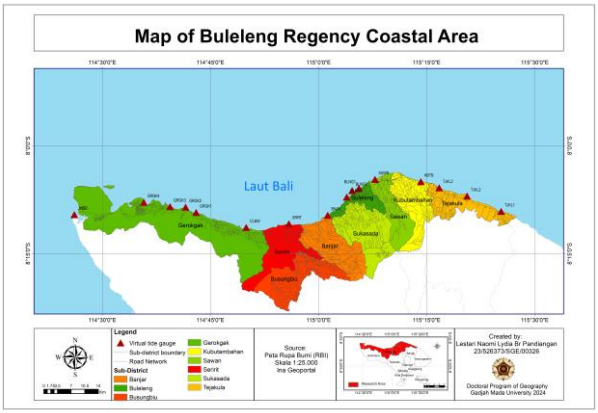

Fig. 3 Research location

The data used in this study are the land surface data, which are collected from the digital elevation model of SRTM DEM, ocean field data collected from DEMNAS, and the fault line data resulting in tsunami [19].

Table 1. Earthquake Source Parameter Data

No	Faults		Thrust Fault
1	Strike (km)		280.954
2	Length (km)		74.47
3	Width (km)		26.54
4	Epicenter	Latitude (o)	7.849
		Longitude (o)	115.23
5	Magnitudo (Mw)		7.5
6	Dip (o)		30
7	Rake (o)		90
8	Depth (km)		10

This study also compared the results from the present work model with the BMKG Indonesian tsunami catalog and supplemented it with a list from

the years 416 and 2018 of the BMKG Tsunami Catalog [19] and PUSGEN 2017 (Table 1).

This research utilizes the 2017 national seismic hazard maps of Indonesia for the Flores Back Arc Plate segment in Bali to constrain the characteristics of the earthquake that generated the tsunami. The epicenter of the earthquake was 7.849°S and 115.23°E, with a focal mechanism of Mw 7.5, fault length of 74.47 km, fault width of 26.54 km, strike of 280.954, dip of 30°, dip of 90°, and slip of 10 km. Then this work developed numerical modeling to track how the tsunami waves travel, when they arrive, how high the waves are, and how far below the Buleleng Regency will be inundated. The National Tsunami Early Warning Center (BMKG) provides three levels of tsunami wave height: MAJOR WARNING (wave height is greater than 3 m), WARNING (wave height is between 0.5 m and 3 m), and ADVISORY (wave height is less than 0.5 m) (Table 2).

Table 2. Wave Height Warning Level for Early Warning

No	Wave Height (meter)	Warning Level
1	> 3	Major Warning
2	0.5 - 3	Warning
3	< 0.5	Advisory

3.2 Tsunami modelling approach

The COMCOT v1.7 (Cornell Multi-grid Coupled Tsunami model) is used in this research to simulate propagation of the tsunami wave, wave height, run-up, arrival time, and inundation at Buleleng Regency.

3.2.1 Definition of tsunami

A tsunami consists of a sequence of waves produced by the abrupt displacement of substantial volumes of water, typically instigated by earthquakes, underwater volcanoes, landslides, or atmospheric and meteorological phenomena [20][21]. These events suddenly elevate sea levels due to seabed deformation or fault movements that displace the overlying water column [22][23]. In contrast to typical ocean waves, the velocity of a tsunami is contingent upon water depth, as articulated in the shallow water wave equation [24].

3.2.2 Terms related to tsunamis

The tsunami inundation parameters on land define several variables, which are called tsunami parameters. These tsunami characters are the significant evidence that could be examined and incorporated in studies of paleotsunami, tsunami modeling, and evacuation route design [25]. The parameters of the tsunami wave from Tsunami Glossary (2019) are shown in Figure 4.

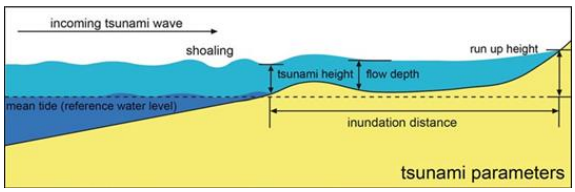

Fig. 4 Tsunami Wave Parameters

3.2.3 Model formulation

COMCOT solves the shallow-water equations. Linear shallow-water equations (LSWE) are applied to tsunami propagation in deep ocean [Eqs. 1–3], while Nonlinear shallow-water equations (NLSWE) are applied in shallow coastal and inundation regions [Eqs. 4–5], with nonlinear and bottom-friction terms included. Variables include surface elevation (η), water depth (h), fluxes (P, Q), Coriolis term (f), and bottom friction terms (Fx, Fy).

Linear Shallow Water Equations (LSWE):

$$\frac{\partial \eta}{\partial t}+\frac{1}{R cos\varphi}\left\{\frac{\partial P}{\partial \psi}+\frac{\partial}{\partial \varphi}(cos\,\varphi Q)\right\}=-\frac{\partial h}{\partial t} \quad (1)$$

$$\frac{\partial P}{\partial t}+\frac{gh}{R cos\varphi}\frac{\partial \eta}{\partial \psi}-fQ=0 \quad (2)$$

$$\frac{\partial Q}{\partial t}+\frac{gh}{R}\frac{\partial \eta}{\partial \psi}+fP=0 \quad (3)$$

Nonlinear Shallow Water Equations (NLSWE):

$$\frac{\partial P}{\partial t}+\frac{1}{R cos\varphi}\frac{\partial}{\partial \psi}\left\{\frac{P^2}{H}\right\}+\frac{1}{R}\frac{\partial}{\partial \varphi}\left\{\frac{PQ}{H}\right\}+\frac{gH}{R cos\varphi}\frac{\partial \eta}{\partial \psi}-fQ+Fx=0 \quad (4)$$

$$\frac{\partial Q}{\partial t}+\frac{1}{R cos\varphi}\frac{\partial}{\partial \psi}\left\{\frac{PQ}{H}\right\}+\frac{1\partial}{R\partial \varphi}\left\{\frac{Q^2}{H}\right\}+\frac{gH}{R}\frac{\partial \eta}{\partial \varphi}+fP+Fy=0 \quad (5)$$

Where:

H = water surface elevation (m)
H = still water depth (m)
H = $\eta+h$ = total water depth (m)
P,Q = volume flux components in the x (east–west) and y (north–south) directions (m^3/s per unit width)
ψ,ϕ = longitude and latitude (degrees)
R = Earth's radius (6,371 km)
G = gravitational acceleration (9.81 m/s^2)
F = Ω sin ϕ = Coriolis parameter due to Earth's rotation (s^{-1}), with Ω = 7.292 × 10^{-5} rad/s
Fx,Fy = bottom friction terms in the x and y directions (m^2/s^2), evaluated using Manning's formula

3.2.4 Boundary conditions

In COMCOT, detailed provisions about boundary conditions are essential for computer simulations that provide a realistic picture of tsunamis. A number of different methods exist for the outermost grid. These include a non-reflecting boundary condition that allows waves to exit the domain

freely; an absorbing boundary condition, in which a sponge layer damps wave energy and reduces reflections; or an input boundary condition where solutions outwith the domain such as FACTS data are prescribed. Waves that reach the input boundary are satisfied to non-reflecting conditions. For inner grids within a nested mesh, boundary conditions are again interpolated between parent-gird sediment and water. To improve stability and eliminate reflections, the enhanced interpolated boundary scheme also employs a sponge layer. These boundary treatments, combined with the shallow water equations and initial conditions, ensure accurate representation of tsunami generation, propagation, and coastal inundation [26].

4. RESULTS AND DISCUSSIONS

4.1 Tsunami wave propagation

In the present work, the tsunami modeling was performed for 60 minutes. Screenshots of outputs of the modeling represent the predicted propagation of tsunami waves for each minute after the earthquake. The tsunami uplift wave is represented by the red arrows, and the tsunami subsidence wave by the blue arrows. An upward wave is one that can arrive at the coast and inundate the tideless area.

The simulation findings show tsunami waves might spread over the Flores Back Arc Thrust after a Mw 7.5 earthquake. Wave energy is also moving to the northern coast of Bali Island, with Buleleng regency getting the most of it.

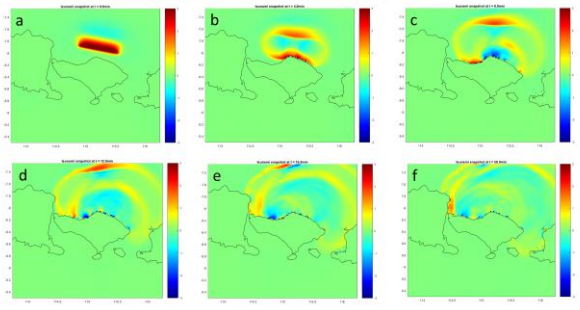

Fig. 5 Tsunami modeling on layer 1 (a) t = 0 minutes, (b) t = 4 minutes, (c) t = 8 minutes, (d) t = 12 minutes, (e) t = 16 minutes, and (f) t = 20 minutes

Figures 5 (a)–(f) show how tsunami waves spread out in the first 20 minutes following the earthquake. At t = 0 min (Figure 5a), the first change in the sea surface happens right after the rupture. The western side of the fault goes up (red), while the eastern side goes down (blue). At t = 4 min (Figure 5b), the first waves start to move outward, mostly to the east and west of the fault. At t = 8 min (Figure 5c), the tsunami waves hit the neighboring shoreline, and the shore starts to show more clearly the alternating crests and troughs. At t = 12 min (Figure 5d), the waves spread out much more over the northern shore of Bali. This illustration shows that incoming and reflected waves are interfering with each other. At t = 16 min (Figure 5e), the coastal wave field develops more complicated because primary waves and reflections from the coastline are interacting with each other. Energy is still moving strongly east and west. Finally, by t = 20 min (Figure 5f), the tsunami has spread out across a larger area, and reflected waves are having a bigger effect on the overall pattern of propagation. Overall, these pictures show how the earthquake caused the seafloor to change, which in turn caused the sea surface to change. This caused uplift and subsidence on opposite sides of the fault and directed tsunami energy mostly eastward and westward, which is what would happen if the fault slipped orthogonal to the strike.

4.2 Tsunami run up and arrival time along the Buleleng coast

The time it takes for a tsunami to reach the Buleleng shoreline area is very different. The eastern shore is the most relevant because the first wave's crest hit this shore less than two minutes after the disturbance.

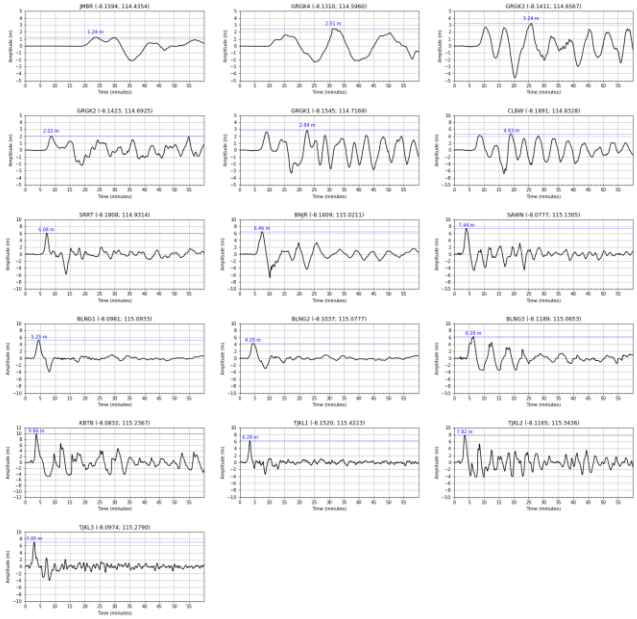

Fig. 6 Tsunami amplitude recorded at 16 observation points during the simulation

Table 3 below displays that most of the sites (12 out of 16) fall in the "Major Warning" category, with run-up over 3 m, indicating very high risk of coastal damage and flooding. Highest run-up occurs at Bukti Beach (9.86 m), followed by Tegal Desa (7.82 m), Ponjok Batu (7.05 m), and Sangit Port (7.44 m). Several other beaches, such as Penimbangan Beach (6.28 m) and Banyuning Beach (5.25 m), are also highly vulnerable.

Table 3. Run-up tsunamis at observation locations

No	Longitude	Latitude	Location	Sib-district	Code of Virtual Tide Gauge	Run-up (meter)	Warning Level
1	115.42	-8.15	Cinta Bulakan Beach	Tejakula	TJKL1	6.28	Major Warning
2	115.34	-8.12	Tegal Desa Beach	Tejakula	TJKL2	7.82	Major Warning
3	115.28	-8.10	Ponjok Batu Beach	Tejakula	TJKL3	7.05	Major Warning
4	115.24	-8.08	Bukti Beach	Kubu Tambahan	KBTB	9.86	Major Warning
5	115.13	-8.08	Sangit Port	Sawan	SAWN	7.44	Major Warning
6	115.09	-8.10	Banyuning Beach	Buleleng	BLNG1	5.25	Major Warning
7	115.08	-8.10	Skip Beach	Buleleng	BLNG2	4.29	Major Warning
8	115.07	-8.12	Penimbangan Beach	Buleleng	BLNG3	6.28	Major Warning
9	115.02	-8.16	Lovina Beach	Banjar	BNJR	6.46	Major Warning
10	114.93	-8.18	Pengastulan Beach	Seririt	SRRT	6.08	Major Warning
11	114.83	-8.19	Celukan Bawang Beach	Gerokgak	CLBW	4.63	Major Warning
12	114.72	-8.15	Gondol Beach	Gerokgak	GRGK1	2.84	Warning
13	114.69	-8.14	Banyu Poh Beach	Gerokgak	GRGK2	2.02	Warning
14	114.66	-8.14	Pemuteran	Gerokgak	GRGK3	3.24	Major Warning
15	114.60	-8.13	Bangsal Port	Gerokgak	GRGK4	2.51	Warning
16	114.44	-8.16	Gilimanuk Port	Gerokgak	JMBR	1.24	Warning

Four locations, however, belong to the "Warning" category with lower run-up values, but no less hazardous due to adjoining settlements and infrastructure: Gondol (2.84 m), Banyu Poh (2.02 m), Bangsal Port (2.51 m), and Gilimanuk Port (1.24 m). In general, the eastern and central coasts (Tejakula, Sawan, Kubu Tambahan) are in the most threat, with the western coast (Gerokgak, Gilimanuk) under lesser but still significant threats.

Table 4. Arrival Times of Tsunami Waves at Observation Locations

No	Longitude	Latitude	Location	Sub-district	Code of Virtual Tide Gauge	Arrival Times (minutes)
1	115.42	-8.15	Cinta Bulakan Beach	Tejakula	TJKL1	2.25
2	115.34	-8.12	Tegal Desa Beach	Tejakula	TJKL2	2.13
3	115.28	-8.10	Ponjok Batu Beach	Tejakula	TJKL3	1.76
4	115.24	-8.08	Bukti Beach	Kubu Tambahan	KBTB	2.50
5	115.13	-8.08	Sangit Port	Sawan	SAWN	2.50
6	115.09	-8.10	Banyuning Beach	Buleleng	BLNG1	2.8
7	115.08	-8.10	Skip Beach	Buleleng	BLNG2	2.8
8	115.07	-8.12	Penimbangan Beach	Buleleng	BLNG3	4.6
9	115.02	-8.16	Lovina Beach	Banjar	BNJR	5.25
10	114.93	-8.18	Pengastulan Beach	Seririt	SRRT	5.5
11	114.83	-8.19	Celukan Bawang Beach	Gerokgak	CLBW	6.8
12	114.72	-8.15	Gondol Beach	Gerokgak	GRGK1	6.96
13	114.69	-8.14	Banyu Poh Beach	Gerokgak	GRGK2	6.96
14	114.66	-8.14	Pemuteran	Gerokgak	GRGK3	8.06
15	114.60	-8.13	Bangsal Port	Gerokgak	GRGK4	10.3
16	114.44	-8.16	Gilimanuk Port	Gerokgak	JMBR	20.04

According to Table 4, tsunamis arrive very differently across Buleleng Regency. In the fastest areas, waves come very quickly. So it takes less then 2 minutes for a big wave to reach Ponjok Batu Beach, less than 2 and a half minutes on average at Tegal Desa Beach or Cinta Bulakan Beach. Such extremely low figures make Tejakula subject to very high risks since evacuations can only start immediately after shaking finishes. Two beaches just to the west (Kubu Tambahan and Sawan's Sangit

Port) both have arrival times of 2.5 minutes or less, which is too short for any meaningful action in response. On the north coast of Buleleng sub-district, Skip Beach and Banyuning Beach are both reached in 2.8 minutes while Penimbangan Beach receives the waves, peaking out at 4.6 minutes before there's only a little more time to run away. Side-stepping into a more western position, tsunamis hitting the shore at Banjar Beach and then Seririt's Pengastulan Beach result in shorter delays in response times. In the Gerokgak area, which lies to the southwest of Buleleng sub-district, arrival times are considerably longer. Reporting times range from 6.8 minutes at Celukan Bawang to about 7 minutes at Gondol and Banyu Poh and then 8 minutes on arrival in Pemuteran. It's a 10.3 minute break at Bangsal Port, while out west, at the most distant point possible, Gilimanuk Port with its longest arrival time of 20 minutes.

4.3 Inundation Extent and Affected Areas

The inundation model shows that low-lying coastal areas are particularly vulnerable to tsunami flooding. Large portions of eastern Buleleng are inundated, while inundation in the central and western sectors is more localized.

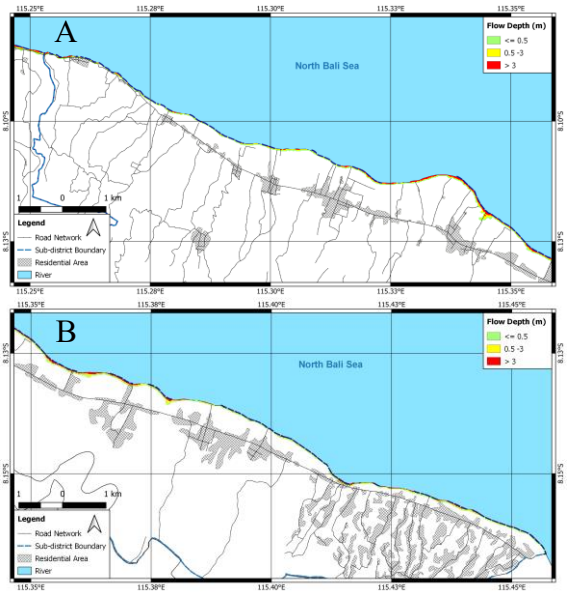

Fig. 7 Tsunami inundation map of Tejakula Sub-District due to Mw 7.5 earthquake: (a) eastern part and (b) western part

As shown in Figure 7, the tsunami flooded the eastern and western parts of the Tejakula sub-district. There are three groups of flooding locations dependent on how deep the flow is. The flow depth in the green category is less than 0.5 meters, in the yellow category it is between 0.5 and 3 meters, and in the red category it is more than 3 meters. The chart shows that most of these flood zones are along the shore of the North Bali Sea, near major communities. Tejakula's tsunami-affected area is about 0.943 km². Most of the affected area is in the shallow inundation zone (< 0.5 meters), which is about 0.472 km² in 1714 grid cells. This means that the highest risk zone (> 3 meters) is widespread but not very deep, with 0.216 km² in 786 cells. These are areas that may be affected the most, especially near the coast.

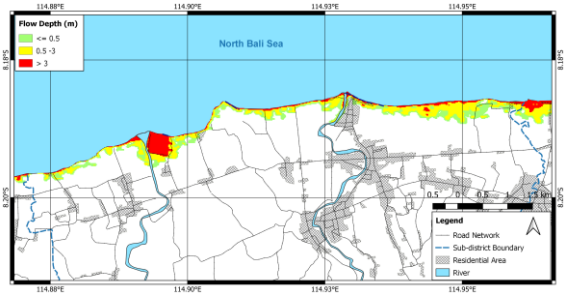

Fig. 8 Tsunami Inundation Map for the Seririt Sub-district due to a Mw 7.5 Earthquake

Figure 8 demonstrates that the flooding from the tsunami in Seririt is largely along the central to eastern coast, notably around river mouths and towns. The entire area impacted is around 1.10 km². The largest region is moderate flooding (0.5–3 m), which covers 0.8208 km² in 2,982 grid cells. The next largest area is shallow flooding (< 0.5 m), which covers 0.2791 km² in 1,014 grid cells. The smallest area is heavy flooding (> 3 m), which covers 0.2163 km² and in 786 grid cells. Seririt is more at risk than Tejakula because the moderate and deep flooding goes deeper inland. This is probably because of the river system and the fact that there are a lot of communities along the coast.

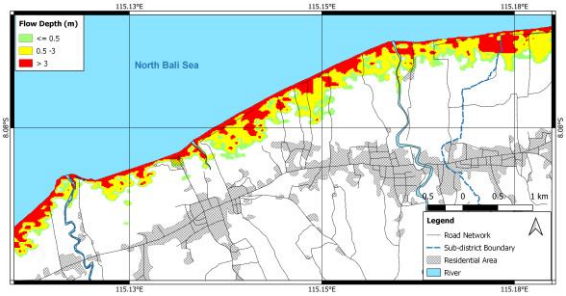

Fig. 9 Tsunami Inundation Map for the Sawan Sub-district due to a Mw 7.5 Earthquake

Figure 9 depicts how the tsunami flooded northern Sawan, encompassing about 1.95 km² (7,100 grid cells). The flooding is split into three areas: shallow (< 0.5 m) with 0.5475 km² (1,989 cells) at the edges, moderate (0.5–3 m) as the largest area with 0.9419 km² (3,422 cells) going inland through river estuaries, and deep (> 3 m) with 0.4649 km² (1,689 cells) near coastal settlements and facilities. In the deep zone, houses, roads and infrastructure are all

rendered insecure. Overall, Sawan's coastal shape combined with its river systems bring an increased risk of tsunamis, highlighting the need for better evacuation routes, land-use control, and disaster-resilient facilities.

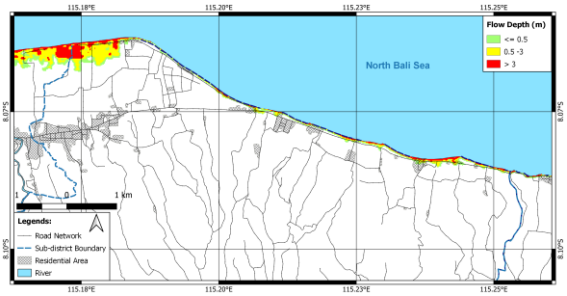

Fig. 10 Tsunami Inundation Map for the Kubu Tambahan Sub-district due to a Mw 7.5 Earthquake

Figure 10 shows tsunami inundation in Kubu Tambahan Sub-district after a Mw 7.5 earthquake, covering about 0.77 km² (2,799 grid cells). The flooding is divided into three zones: shallow (< 0.5 m) with 0.2461 km² (894 cells) scattered along the coast, moderate (0.5–3 m) as the largest zone with 0.3523 km² (1,280 cells), and deep (> 3 m) covering 0.1720 km² (625 cells), concentrated in low-lying coastal settlements. mostly nearshore occurrences are reflected on the map while the highest hazard zones are depicted red at the northwest and northeast coastal parts.

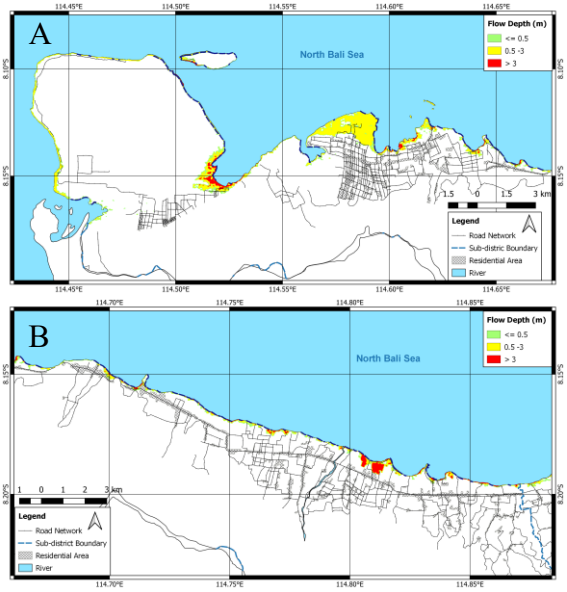

Fig. 11 Tsunami Inundation Map for the Gerokgak Sub-District Mw 7.5 earthquake: (a) eastern part and (b) western part

Figure 11 reveals that Gerokgak is the most devastated sub-district, with around 8.87 km² (32,217 grid cells) of land being covered by the tsunami. There are deep floods surrounding the bay and river estuary in the west, and lengthy, narrow flood courses with many deep zones near heavily inhabited areas in the east. There are three levels of flooding: shallow (< 0.5 m), which affects 8,920 cells (2.37 km²); moderate (0.5–3 m), which affects 13,720 cells (5.36 km²); and deep (> 3 m), which affects 9,577 cells (1.14 km²). In Buleleng, the coastal lowlands and communities of Gerokgak are the most at risk from tsunamis.

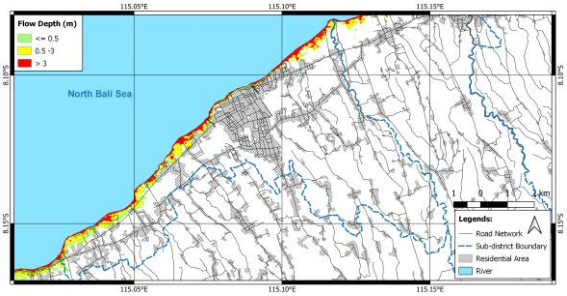

Fig. 12 Tsunami Inundation Map for the Buleleng Sub-district due to a Mw 7.5 Earthquake

Figure 12 shows that the tsunami inundation significantly penetrates inland into the coastal plains, especially in the heavily populated mid-areas of the sub-district. Flooding is to be expected on bends along the coast and at river mouths, with the red areas representing the deepest inundation. The green area (coastal) is represented as a thin layer outside the settlement area, and the yellow one (inland) wraps around the center of the settlement. Total direct flood extent is about 2.67 km² (9,709 grid cells). Shallow (less than half a meter) inundation impacts 3,142 grid cells (covering 0.86 km²), moderate (0.5 to 3) inundation hits 4,446 grid cells (covering 1.22 km²), and deep (in excess of 3 meters) inundation affects 2,121 grid cells (covering 0.58 km²).

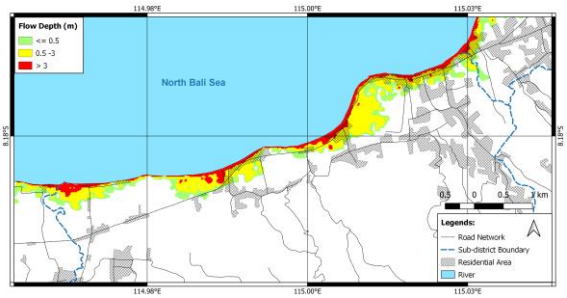

Fig. 13 Tsunami Inundation Map for the Banjar Sub-district due to a Mw 7.5 Earthquake

Figure 13 shows a continuous stretch of flooding along the coast. The area with the highest depth, indicated by the red zone, is located around lowland settlements and near the estuary. The shallow zone (green) is spread along the coastline. The medium-depth zone (yellow) dominates most of the affected coastline and extends inland to densely populated

areas. Data shows that the impact of flooding covers a total of 2.11 km², consisting of 7,654 grid cells. The inundation is divided into three depth categories: shallow inundation (≤ 0.5 meters) impacts 2.289 grid cells. covering 0.63 km²; moderate inundation (0.5–3 meters) affects 4.333 grid cells. totaling 1.19 km²; and deep inundation (> 3 meters) occurs in 1.032 grid cells. spanning 0.28 km².

4.4 Population and Land Use Exposure

Overlaying inundation map with population and landuse shows high density populated clusters and critical facilities (infrastructure) in low lying area are directly hit by tsunami. This demonstrates some of the potential for significant social and economic impacts if no action is taken.

Table 5. The tsunami inundation area based on flood depth for each sub-district

No	Sub-district	Shallow (km^2)	Moderate (km^2)	Deep (km^2)	Total Inundation Area (km^2)
1	Banjar	0.63	1.19	0.28	2.11
2	Buleleng	0.86	1.22	0.58	2.67
3	Gerokgak	2.46	5.28	1.14	8.87
4	Kubu Tambahan	0.25	0.35	0.17	0.77
5	Sawan	0.55	0.94	0.46	1.95
6	Seririt	0.67	0.82	0.28	1.77
7	Tejakula	0.47	0.26	0.22	0.94
	Total	5.89	10.06	3.14	19.09

Information on tsunami inundation depth at seven sub-districts is provided in Table 5. Inundation depth is divided into three classes: ≤0.5 m, >0.5–≤3.0 m, and >3.0 m. Gerokgak has the largest flooding size at all inundation depths, covering about 8.87 km². Buleleng and Banjar are ranked next with 2.67 km² and 2.11 km² of total inundation area, respectively. Tejakula has the least area inundated, at the size of 0.94 km². In total, 10.06 km² is occupied by the tsunami inundation, which is mainly within the accommodation range of 0.5-3.0 m after taking all areas into account. and 5.89 km² in the less than 0.5 m category and 3.14 km² in the more than 3.0 m category. The result suggests that water with a moderate level of inundation (0.5–3.0 m) is the most vulnerable, especially in the Gerokgak area, with a high probability of tsunami.

4.5 Discussion

The models in this study reveal that the eastern section of Buleleng will be affected by a tsunami in less than two minutes, which is not enough time for people to to evacuate horizontally. This finding is consistent with previous research, which indicated that in Padang Barat, a brief evacuation period significantly impeded horizontal evacuation [27]. Similar to Padang, this study findings suggest that Buleleng should prioritize vertical evacuation, particularly in densely populated lowland regions.

The modeled run-up heights at Buleleng, which can reach 3.4 m in certain locations, show that there is a substantial chance of major coastal flooding. Similar studies at Pacitan Bay, which indicated bottlenecks along evacuation routes in tsunami modeling, this study demonstrate that effective evacuation planning in Buleleng must account for the limited warning time and the local traffic capacity in coastal areas [28]. This also means that safe zones shouldn't be easy to go to in a short amount of time.

This research indicates that Designated Evacuation Buildings in Buleleng must endure both seismic and hydrodynamic tsunami forces. Previous evaluations have shown that even reinforced concrete structures in Padang, which meet the earthquake resistance standards, may fail under tsunami forces [29]. This comparison suggests that the current public buildings in Buleleng require evaluation and fortification to function successfully as vertical evacuation shelters.

The flooding at Buleleng, where significant portions of lowland beaches are inundated, is in line with research linking land-use change to increased tsunami vulnerability [30]. In the same way, the urbanization of Buleleng is not as obvious, but the tourism infrastructure along the beaches makes at-risk flooding zones more likely to be hit.

Finally, this study's combination of tsunami modeling and spatial vulnerability assessment is similar to approaches that combine run-up modeling with coastal vulnerability mapping in Bali [31]. The novelty lies in focusing on the Flores Back Arc Thrust as the source of the tsunami, which has never been done previously. To lower the danger of disasters in North Bali, it's important to identify areas with the shortest warning time and the biggest run-up.

5. CONCLUSION

In this research, tsunami hazard in Buleleng Regency is evaluated using COMCOT v1.7 for an Mw 7.5 event on the Flores Back Arc Thrust. The findings reveal marked regional differences in the effects of tsunamis related to local coastal geomorphology and distance from the source. Extremely critical on the eastern coast, where the arrival time of tsunami waves is less than two minutes at Tejakula (Ponjok Batu Beach 1.46 min, Tegal Desa Beach 2.08 min, Cinta Bulakan Beach 2 min), etc. Such very short lead times allow for little or no time for horizontal evacuation. In spatial

extent, inundation is largest in Gerokgak (8.87 km²), followed by Buleleng (2.67 km²), Banjar (2.11 km²), Sawan (1.95 km²), and Seririt (1.77 km²). Despite having a smaller submergence area (0.94 km²), Tejakula is especially vulnerable due to its short warning time. The simulation indicates that Bukti Beach (Kubu Tambahan) has the highest run-up (9.86 m) making it the most at-risk location in the study area, followed by Tegal Desa Beach (7.82 m), Ponjok Batu Beach (7.05 m), Sangit Port in Sawan (7.44 m), and Lovina Beach in Banjar (6.46 m). These results display the magnitude and application of tsunami threats along the coast of Buleleng.

When the maps are superimposed over population and land use data, they show densely populated villages, vital infrastructure installations, and tourism facilities in low-lying areas are at significant risk to both communities and the regional economy. As a result, vertical evacuation and structural strengthening of selected shelters have been emphasized. Furthermore, tsunami hazard maps should be incorporated in spatial planning and coastal development policies to avoid further exposure. By regarding the Flores Back Arc Thrust as a tsunami source, this research introduces discussion of tsunamigenic potential in North Bali and provides scientific information to Buleleng Regency for disaster risk reduction, evacuation planning, and community preparedness.

6. ACKNOWLEDGMENTS

The authors thank to the Indonesian Agency for Meteorology, Climatology and Geophysics (BMKG) and the Faculty of Geography Universitas Gadjah Mada for supporting this research as part of the academic cooperation program that began in 2023.

7. REFERENCES

[1] Bock Y., Prawirodirdjo L., Genrich J. F., Stevens C. W., McCaffrey R., Subarya C., Puntodewo S. S. O., and Calais E., Crustal motion in Indonesia from Global Positioning System measurements, Journal of Geophysical Research, vol. 108, no. B8, 2003, pp. 1-21. https://doi.org/10.1029/2001JB000324

[2] Hamilton W., Tectonics of the Indonesian Region, Bulletin of the Geological Society of Malaysia, vol. 6, 1973, pp. 3–10. https://doi.org/10.7186/bgsm06197301

[3] Kongko W., and Schlurmann T., “the Java Tsunami Model: Using Highly-Resolved Data To Model the Past Event and To Estimate the Future Hazard,” Coastal Engineering Proceedings, no. 32, 2011, pp. 25. https://doi.org/10.9753/icce.v32.management.25

[4] Central Agency of Statistics, ISSN: 0215-5389, Kabupaten Buleleng Dalam Angka 2023, Badan Pusat Statistik, 2023, pp. 1-268.

[5] Mardiatno D., Malawani M. N., and Nisaa R. M., The future tsunami risk potential as a consequence of building development in Pangandaran Region, West Java, Indonesia, International Journal of Disaster Risk Reduction, Volume 46, 2020, 101523, ISSN 2212-4209,.pp.1-8. https://doi.org/10.1016/j.ijdrr.2020.101523

[6] Usman F., Saifuddin C., Usman F., Fathoni M., Rozikin M., Saputra H., Murakami K., Assessing coastal population capacity in Tsunami-prone areas: A grid-based approach, Jàmbá: Journal of Disaster Risk Studies, vol. 16,no.1,2024,pp.1-10. https://doi.org/10.4102/jamba.v16i1.1685

[7] Demets C., Gordon R. G., and Donald A. S. S. F., Effect Of Recent Revisions To The Geomagnetic Reversal Time Scale On Estimates Of Current Plate Motions, Journal of Geophysical Research, vol. 15, no. 6, 1994, pp. 1-13. https://doi.org/10.1029/94GL02118

[8] Daryono., Identifikasi sesar naik busur belakang (back arc thrust) daerah Bali berdasarkan seismisitas dan solusii bidang sesar, Artikel Kebumian, Badan Meteorologi Klimatologi dan Geofisika, 2011, pp. 1-4.

[9] PUSGEN, Laporan Pusat Studi Gempa Nasional (Indonesia), Pusat Penelitian dan Pengembangan Perumahan dan Permukiman (Indonesia). 2017, pp. 1-400.

[10] Nguyen N., Griffin J., Cipta A., and Cummins P. R., Indonesia’s Historical Earthquakes: Modelled examples for improving the national hazard map, Record Series, Geoscience Australia, Canberra, 2015, pp. 115-116. https://doi.org/10.11636/Record.2015.023

[11] Sianipar D. S. J., Huang B. S., Ma K. F., and Chen P. F., Taiwan International Ph.D. Graduate Program for Earth System Science (TIGP-ESS) Earthquake Source Characteristics along the Flores Thrust Fault, Indonesia 研究生, no. June, 2022, pp. 1-207.

[12] Amri M. R., Yulianti G., Yunus R., Wiguna S., Adi A. W., Ichwana A. N., Randongkir R. E., Septian R T., Risiko Bencana Indonesia, BNPB, 2016, pp. 272-273.

[13] Sambah A. B., and Miura F., Integration of Spatial Analysis for Tsunami Inundation and Impact Assessment, Journal of Geographic Information Systems, vol. 06, no. 01, 2014, pp. 11–22. https://doi.org/10.4236/jgis.2014.61002

[14] Marfai M. A., King L., and Singh L., Natural hazards in Central Java Province, Indonesia: An overview, Environmental Geology, vol. 56, no. 2, 2008, pp. 335–351. https://doi.org/10.1007/s00254-007-1169-9

[15] Bakar A. A., Mardiatno D., and Marfai M. A., Study on potential tsunami by earthquake in subduction zone of Sulawesi Sea, Arabian Journal of Geosciences, vol. 10, no. 24, Dec. 2017, pp. 2-3. https://doi.org/10.1007/s12517-017-3286-4

[16] Annisa D. N., Mardiatno D., and Hizbaron D. R., Pengelolaan Wilayah Pesisir Berbasis Pengurangan Risiko Bencana Gempabumi dan Tsunami di Kabupaten Kulon Progo Daerah Istimewa Yogyakarta, Journal of Civil Engineering and Planning, vol. 2, no. 1, 2021, pp.1–19. https://doi.org/10.37253/jcep.v2i1.4262

[17] Roger J., Pelletier B., and Gusman A., Power W., Wang X., Burbidge D., and Duphil M., Potential tsunami hazard of the southern Vanuatu subduction zone: Tectonics, case study of the Matthew Island tsunami of 10 February 2021 and implication in regional hazard assessment, Natural Hazards and Earth System Sciences, vol. 23, no. 2, 2023, pp. 393–414. https://doi.org/10.5194/nhess-23-393-2023

[18] Mardiatno D., Malawani M. N., Wacono D., and Annisa D. N., Review on Tsunami Risk Reduction in Indonesia Based on Coastal and Settlement Typology, Indonesian Journal of Geography, vol. 49, no. 2, Nov. 2017. pp. 186–194. https://doi.org/10.22146/ijg.28406

[19] BMKG, Katalog Tsunami Indonesia Tahun 416-2018. ISSN 978-602-50542-9-7, 2019.

[20] Setyahagi A. R., Pemodelan Tsunami di Pantai Sendang Biru Kabupaten Malang, Sekolah Tinggi Meteorologi Klimatologi dan Geofisika, 2017.

[21] Bryant E., Tsunami: The Underrated Hazard, Springer, vol. 82, no. 48, 2008, pp. 588. https://doi.org/10.1029/01EO00342

[22] IOC-UNESCO, Tsunami Glossary, Technical Series 85, Intergovernmental Oceanographic Commission ., 2019, pp. 1-46

[23] Leschka S., Pedersen C., and Larsen O., On the requirements for data and methods in tsunami inundation modelling – Roughness map and uncertainties, Water, Volume 1, May 2011, 2009, pp 1-8.

[24] Kanamori H., Mechanism of tsunami earthquakes, Physics of the Earth and Planetary Interiors, vol. 6, no. 5, 1972, pp. 346–359. https://doi.org/10.1016/0031-9201(72)90058-1.

[25] Muqoddas M. M, Pengaruh kekasaran Manning terhadap pemodelan inundasi di Cilacap, Sekolah Tinggi Meteorologi Klimatologi dan Geofisika, 2018, pp. 470–470.

[26] Wang X., COMCOT User Manual Ver. 1.7, Cornell University, vol. 6, 2009, pp. 1–59.

[27] Rifwan F., Andreas L. O., Ashar F., Zola P., and Arifin A., Analysis Of Time And Distance Factors In Tsunami Evacuation Transportation Planning In Padang , West Sumatra, International Journal of GEOMATE, vol. 29, no. 132, 2025, pp. 90–97. https://doi.org/10.21660/2025.132.4975

[28] Jumadi J., Priyono K. D., Sasmi A.T., Saputra A., and Gomez C., Multi-Scenarios Tsunami Hazard And Evacuation Routes Using Seismic Data In Pacitan Bay, Indonesia, International Journal of GEOMATE, vol. 26, no. 116, 2024, pp. 46–53. https://doi.org/10.21660/2024.116.4314

[29] Fauzan., Ikhwan F. M., Nugraha M. D. A., Syandriadji D., and Al Jauhari Z., The Effect of Tsunami Loads on the Prayoga Foreign Language College Building in Padang City, Indonesia, International Journal of GEOMATE, vol. 25, no. 112, 2023, pp. 115–122. https://doi.org/10.21660/2023.112.s8624

[30] Kartika F. D., Muryani C., and Noviani R., Estimated Impact of Tsunami Hazards Due To Urbanization in the Aerotropolis Area of Yogyakarta International Airport, Indonesia, International Journal of GEOMATE, vol. 26, no. 116, 2024, pp. 54–63. https://doi.org/10.21660/2024.116.4346

[31] Sambah A. B., Masnagari L. M. S., Fuad M. A. Z., and Intyas C. A., Tsunami Run-Up Modelling In Comparison With Coastal Vulnerability Mapping, International Journal of GEOMATE, vol. 27, no. 119, 2024, pp. 10–17. https://doi.org/10.21660/2024.119.4000